

1 **Soil-atmosphere exchange of carbonyl sulfide in Mediterranean**
2 **citrus orchard**

3 Fulin Yang#, Rafat Qubaja, Fyodor Tatarinov, Rafael Stern, and Dan Yakir*

4

5 Earth and Planetary Sciences, Weizmann Institute of Science, Rehovot 76100, Israel

6

7 *#Present address:* College of Animal Sciences, Fujian Agriculture and Forestry

8 University, Fuzhou 350002, China

9

10 **Correspondence:* Dan Yakir; email: dan.yakir@weizmann.ac.il

11

12 **Abstract:**

13 Carbonyl sulfide (COS) is used as a as a tracer of CO₂ exchange at the ecosystem
14 and larger scales. The robustness of this approach depends on knowledge of the soil
15 contribution to the ecosystem fluxes, which is uncertain at present. We assessed the
16 spatial and temporal variations of soil COS and CO₂ fluxes in the Mediterranean citrus
17 orchard combining surface flux chambers and soil concentration gradients. The spatial
18 heterogeneity in soil COS exchange indicated net uptake below and between trees of
19 up to -4.6 pmol m⁻² s⁻¹, and net emission in sun exposed soil between rows, of up to
20 +2.6 pmol m⁻² s⁻¹, with a mean uptake value of -1.10 ± 0.10 pmol m⁻² s⁻¹. Soil COS
21 concentrations decreased with soil depth from atmospheric levels of ~450 to ~100 ppt
22 at 20 cm depth, while CO₂ concentrations increased from ~400 to ~5000 ppm. COS
23 flux estimates from the soil concentration gradients were, on average, -1.02 ± 0.26 pmol
24 m⁻² s⁻¹, consistent with the chamber measurements. A soil COS flux algorithm driven
25 by soil moisture and temperature (5 cm depth) and distance from the nearest tree, could
26 explain 75% of variance in soil COS flux. Soil relative uptake, the normalized ratio of
27 COS to CO₂ fluxes was, on average -0.37 and showed a general exponential response
28 to soil temperature. The results indicated that soil COS fluxes at our study site were
29 dominated by uptake, with relatively small net fluxes compared to both soil respiration
30 and reported canopy COS fluxes. Such result should facilitate the application of COS
31 as a powerful tracer of ecosystem CO₂ exchange.

32

33 **Keywords:**

34 Carbonyl sulfide; COS; OCS; soil gas exchange; ecosystem gas exchange; tracer of
35 carbon fluxes.

36 **1. Introduction**

37 Carbonyl sulfide (COS) is a Sulphur-containing analogue of CO₂ that is taken up
38 by vegetation following a similar pathway to CO₂, ultimately hydrolyzed in an
39 irreversible reaction with carbonic anhydrase. It therefore holds great promise for
40 studies of photosynthetic CO₂ uptake (Asaf et al., 2013; Berry et al., 2013; Wehr et al.,
41 2017; Whelan et al., 2018). One of the difficulties in the application of COS as a tracer
42 for photosynthetic CO₂ uptake is that the non-leaf contributions to the net ecosystem
43 COS flux are poorly characterized. There are reports of substantial soil fluxes,
44 indicating both uptake and emissions (Kesselmeier et al., 1999; Kuhn et al., 1999;
45 Masaki et al., 2016; Seibt et al., 2006; Yang et al., 2018; Yi et al., 2007). Although soil
46 COS exchanges were in some cases small compared to plant uptake (e.g., Yang et al.,
47 2018; Berkelhammer et al., 2014), this was not always the case. Substantial soil COS
48 emissions have been found in wetlands and anoxic soils (Li et al., 2006; Whelan et al.,
49 2013), and in senescing agricultural fields and high temperatures (Liu et al., 2010;
50 Maseyk et al., 2014), or under drought conditions and in response to UV radiation (Kitz
51 et al., 2017). Even for the same soil, COS fluxes could show large variations and both
52 uptake and emission with sensitivities to soil moisture, and ambient COS
53 concentrations (Bunk et al., 2017; Kaisermann et al., 2018). These studies also assessed
54 the response of COS exchange to environmental controls, e.g. soil moisture and
55 temperature and solar radiation.

56 For COS application as a tracer of ecosystem CO₂ exchange characterizing the
57 relationships between COS and CO₂ fluxes is important. This is done by assessing the
58 'relative uptake' (RU) of the COS/CO₂ flux rate ratio, normalized by the ambient
59 atmospheric concentrations (that differ for the two gases by a factor of about 10⁶), as
60 done at the leaf scale, (LRU) or ecosystem scale (ERU; e.g, Asaf et al., 2013). It was
61 similarly applied to soil as SRU (Berkelhammer et al., 2014). Conservative, or
62 predictable, SRU values reflect systematic relationships between the processes
63 influencing CO₂ and COS, could help the identification of the dominant process, and
64 support the application of COS as tracer. Small SRU values compared to LRU could
65 also indicate reduced effect of soil on ecosystem fluxes. For example, Berkelhammer

66 et al. (2014) reported mean SRU of -0.76, which are about half of the leaf values of
67 about +1.7 indicating that compared to CO₂, leaf COS is enhanced, and soil COS uptake
68 is suppressed, which provides additional robustness to the COS-GPP approach. Note
69 also that as soil CO₂ flux measurements and modeling are much more common than for
70 COS at flux sites. Knowledge of SRU could help derive soil COS fluxes and, for
71 example, improve the partitioning of canopy COS flux from NEE_{COS} measurements.

72 Soil COS exchange has often been measured by incubations in the lab (e.g., Bunk
73 et al., 2017; Kesselmeier et al., 1999; Liu et al., 2010; Van Diest and Kesselmeier, 2008),
74 and by static or dynamic chambers in the field (e.g., Berkelhammer et al., 2014; Kitz et
75 al., 2017; Sun et al., 2018; Yi et al., 2007; Mseyk et al., 2014), and using models (e.g.,
76 Ogée et al., 2016; Sun et al., 2015; Whelan et al., 2016). In spite of these efforts, more
77 field measurements of soil COS exchange are clearly needed as a basis for elucidating
78 underlying mechanism, as well as obtaining better quantitative record of the possible
79 range of soil COS fluxes under natural conditions. Note also that previous studies have
80 focused on agricultural soils (Maseyk et al., 2014), wetlands (Whelan et al., 2013),
81 boreal forest soils (Sun et al., 2018), and grasslands (Kitz et al., 2017), but several
82 ecosystems are understudied, such as in the Mediterranean. Finally, soil profile
83 measurements will also be useful for validation of soil models of COS exchange (Sun
84 et al., 2015). The objective of this study was to apply dynamic chambers measurements,
85 constrained by simultaneous soil gradient method to assess the spatial and temporal
86 variations soil COS and CO₂ fluxes in a citrus orchard ecosystem where contrasting soil
87 microsite conditions occur.

88

89 **2. Materials and methods**

90 **2.1 Field site**

91 The study was conducted in an orchard in Rehovot, Israel (31°54' N, 34°49' E, 50
92 m, asl) in 2015 and 2016. The orchard is a plantation of lemon trees (*Citrus limonia*
93 *Osbeck*), with 5 m distance between rows and 4 m between trees. Mean annual air
94 temperature at the site is 19.7 °C, and mean annual precipitation is 537 mm. Most of
95 the precipitation (82%) falls in November to February with no rain during June to

96 October. A trickle irrigation system was used from May to September with the standard
97 irrigation plan of the orchard management. The soil in the area is brown red sandy soil
98 (hamra soil) with an average bulk density of 1.6 kg m^{-3} and pH of 6.5 (Singer, 2007).
99 Although root distribution was not measured we noted that roots were concentrated
100 mainly within about 50 cm of the tree trunks, as could be expected due to drip irrigation
101 installed around the trunk.

102

103 **2.2 Quantum cascade laser measurements**

104 We used the commercially available quantum cascade laser (QCL) system
105 (Aerodyne Research, Billerica, MA) with tunable laser absorption spectrometer (Model:
106 QC-TILDAS-CS) to measure COS, CO₂, and water vapor concentrations
107 simultaneously. The device was installed in a mobile lab, described by Asaf et al. (2013).
108 COS is detected at 2050.40 cm^{-1} and CO₂ at 2050.57 cm^{-1} at a rate of 1 Hz. The
109 instrument was calibrated using working reference compressed air tank that was used
110 for inter-comparison with the NOAA GMD lab (Boulder CO). Corrections for water
111 vapor were made using the TDLWINTTEL software installed in the QCL (Kooijmans et
112 al. 2016)

113

114 **2.3 Soil chamber flux measurements**

115 Custom-made stainless-steel cylindrical chamber of 177 cm^2 directly inserted into
116 the soil ($\sim 5 \text{ cm}$) was used, as previously described (Berkelhammer et al., 2014; Yang et
117 al., 2018). The chambers were opaque and photoproduction was not considerate in this
118 study. The chamber air and ambient air flows were pumped to the QCL analyzer through
119 two 3/8-inch diameter Decabon tubing. Flow rate was maintained at 1.2 L min^{-1} and
120 repeatedly cycled with 1 min instrument background (using N₂ zero gas), 9 min ambient
121 air flow, and 10 min chamber air sample. Three different soil sites were used with
122 distance of 3.20, 2.00 and 0.25 m away from a tree trunk, that represented sampling
123 sites between rows (BR), between trees (BT) and under tree (UT). Each sampling site
124 was measured continuously for 24 hours and cycled between sites for the duration of
125 the campaign. Four measurement campaigns were carried out during 5th~9th August

126 2015; 25th~28th December 2015; 5th~9th May 2016; 28th~31th July 2016.

127 Gas exchange rates, F_c , were calculated according to:

128
$$F_c = \frac{Q}{A} \times (\Delta C_{sample} - \Delta C_{blank}) \quad (1)$$

129 where Q is the chamber flush rate in mol s^{-1} ; A is the enclosed soil surface in m^2 ; ΔC is
130 the gas concentrations difference between chamber air and ambient air in pmol mol^{-1}
131 for COS and $\mu\text{mol mol}^{-1}$ for CO_2 under sampling, and blank reference treatments (using
132 the same chamber placed above a sheet of aluminum foil before and after measurement
133 at each site. Hereafter, the soil fluxes are reported in $\text{pmol m}^{-2} \text{s}^{-1}$ and $\mu\text{mol m}^{-2} \text{s}^{-1}$ for
134 COS and CO_2 , respectively. Soil relative uptake (SRU) is used to characterize the
135 relationship between soil CO_2 and COS fluxes, was estimated from the normalized ratio
136 of CO_2 respiration to COS uptake (negative values) or emission (positive values) fluxes
137 (Berkelhammer et al., 2014):

138
$$SRU = \frac{F_{COS_{soil}}}{[COS]} \Big/ \frac{F_{CO_2_{soil}}}{[CO_2]} \quad (2)$$

139

140 **2.4 Soil concentration profile measurements**

141 Four campaigns of soil concentration profile measurements were carried out
142 during 1st~2nd March; 20th~26th April; 10th May; 22nd~28th June of 2016. The trace
143 gas at five soil depths of 0, 2.5, 5.0, 10, 20 cm was sampled at each of the three
144 microsites, BR, BT and UT.

145 Four individual Decabon tubes were inserted at adjacent but different points into
146 the soil (to avoid communication between tubes during sampling), to the different
147 depths indicated above and connected directly to the QCL positioned close by the
148 mobile lab. At least one day after insertion and insuring sealing between tubing and soil,
149 soil air was sampled with flow rate of 80 ml min^{-1} , in a 10 min cycle of 1 min instrument
150 background, 3 min surface air (depth 0; used initially to flush all above ground tubing),
151 5 min sampling of a depth point in the profile (first two minutes for flushing the tubing,
152 third minute used for data; up to 400 ml extracted from the soil), ending with 1 min
153 surface air. Five complete sets of cycles including the four soil depths and surface air

154 were repeated for each site (with time gaps between cycles of hours, and in some cases
155 overnight). The pressure in the 500 ml QCL sample cell was kept at 15 torr to insure
156 sufficient turnovers (~8 per minute using the low flow rate) before data were recorded.

157 Assuming that in the selected measurement sites, soil trace gas is only
158 transported by diffusion, soil COS and CO₂ fluxes were estimated based on the Fick's
159 first law:

$$160 \quad F = -D_s \frac{dC}{dz_{soil}} \quad (3)$$

161 where F is the upward or downward gas flux (pmol m⁻² s⁻¹ for COS and μmol m⁻² s⁻¹
162 for CO₂); D_s is the effective gas diffusion coefficient of the relevant gas species in the
163 soil (m² s⁻¹); C the trace gas concentration (mixing ratio, converted from the measured
164 mole fractions); z_{soil} is the soil depth (m).

165 The Penman (1940) function was used to describe the soil diffusion coefficient
166 (D_s) as in Kapiluto et al. (2007):

$$167 \quad D_s = D_a (\theta_s - \theta) \sqrt{\frac{T_s + 273.15}{298.15}} \quad (4)$$

168 where θ_s is the soil saturation water content and θ is the measured soil volumetric water
169 content. D_a is the trace gas diffusion coefficient in free air, which varied with
170 temperature and pressure, given by

$$171 \quad D_a = D_{a0} \left(\frac{T_s + 273.15}{293.15} \right)^{1.75} \left(\frac{P}{101.3} \right) \quad (5)$$

172 where D_{a0} is a reference value of trace gas diffusion coefficient at 293.15 K and 101.3
173 kPa, given as 1.24×10^{-5} m² s⁻¹ for COS (Seibt et al., 2010) and 1.47×10^{-5} m² s⁻¹
174 for CO₂ (Jones, 1992); T_s is soil temperature (°C), and P is air pressure (kPa).

175

176 **3. Results**

177 **3.1 Variations in soil COS flux**

178 Soil COS fluxes showed significant heterogeneity at both the spatial (microsites)
179 and temporal (seasonal) scale (Fig. 1). Overall, the hourly soil COS flux varied from -
180 4.6 to +2.6 pmol m⁻² s⁻¹, with mean value of -1.10 ± 0.10 pmol m⁻² s⁻¹. On the spatial

181 scale, the COS fluxes showed systematically uptake under trees (UT), moderate uptake
182 and some emissions between trees (BT) and relatively more emission in the exposed
183 area between rows (BR), with diurnal mean values across seasons of -3.00 ± 0.10 , -0.43
184 ± 0.13 and $+0.13 \pm 0.11$ $\text{pmol m}^{-2} \text{s}^{-1}$, respectively.

185 On the diurnal time-scale, soil COS flux were generally higher in the afternoon
186 (peaking around 15:00~16:00 hours), declining at night and early morning (Fig. 1). On
187 the seasonal time scale, soil COS fluxes showed both changes in rates and shifts from
188 net uptake to net emission, with the site hierarchy differing in the different seasons (Fig.
189 1). In the UT site where only COS uptake was observed, the highest rates were observed
190 in winter and peak summer (December and August) with diurnal mean rates of nearly
191 -4 $\text{pmol m}^{-2} \text{s}^{-1}$, and more moderate uptake rates, around -2 $\text{pmol m}^{-2} \text{s}^{-1}$, in spring and
192 early summer (May and July; Fig. 1). In the BT sites, significant COS uptake of ~ 2.5
193 $\text{pmol m}^{-2} \text{s}^{-1}$ was observed in winter, but net fluxes were near zero in other times, with
194 some afternoon emission in summer. In the exposed BR sites, minor uptake (less than
195 -1 $\text{pmol m}^{-2} \text{s}^{-1}$) was observed in spring and early summer, but consistent emission in
196 peak summer, with diurnal mean values of nearly $+2$ $\text{pmol m}^{-2} \text{s}^{-1}$.

197

198 **3.2 Effects of moisture and temperature**

199 During the hot summer (August 2015 and July 2016), differences in microsite soil
200 water content (θ) were most distinct, with θ of nearly 30% in the UT sites (associated
201 with drip irrigation), but $\sim 19\%$ and $\sim 12\%$ in the BT and BR sites. Correspondingly, the
202 UT sites had significant COS uptake of about -3 $\text{pmol m}^{-2} \text{s}^{-1}$ while the other sites
203 showed emission of about $+1$ $\text{pmol m}^{-2} \text{s}^{-1}$ (Table 1). In winter (December), θ in the
204 three sites was similar, $\sim 25\%$, and all sites showed soil COS uptake, but with clear
205 gradient of -3.9 , -2.5 and -0.7 $\text{pmol m}^{-2} \text{s}^{-1}$ in the UT, BT and BR sites, respectively (Fig.
206 1). On average, soil COS fluxes showed non-linear increase in uptake with increasing
207 θ , but it seems that this response may saturate at about θ of 25% and uptake rates of \sim
208 3.9 $\text{pmol m}^{-2} \text{s}^{-1}$ (Fig. 2). The fit to the data presented in Fig. 2 also indicate that in dry
209 soil with $\theta < 15\%$ soil COS emission can be expected.

210 The response of soil COS fluxes to soil temperature varied among the three

211 measurement sites (Fig. 3). The BT and BR sites showed a near linear response with a
212 shift from uptake to emission around 25 °C. In the shaded and moist UT site, COS uptake
213 was always significant ranging between -4 to -1 pmol m⁻¹ s⁻¹ with relatively low
214 temperature sensitivity, and with lowest mean uptake rates around 20 °C.

215 Pearson product-moment correlation analysis results showed that hourly soil COS
216 flux was significantly related to soil moisture and temperature (at the 0.001 level), and
217 the soil moisture had a stronger environmental controls on the soil COS flux ($r=-0.77$),
218 compared with soil temperature ($r=+0.45$).

219 Comprehensive assessment of the effects of soil moisture (θ), temperature (T_s) and
220 distance away from tree trunk (d), showed that hourly soil COS flux (F_{COS}) could be
221 fitted to a three parameters exponential model, which could explain 75% of the
222 variation in soil COS flux (Eq. 6).

$$223 \quad F_{COS} = 8.91 \exp(0.01T_s - 0.01\theta + 0.09d - 0.33) - 8.86, \quad R^2 = 0.75 \quad (6)$$

224

225 3.3 COS flux estimates from soil concentration gradients

226 The average soil concentration gradient of COS and CO₂ for the four campaigns
227 is shown in Fig. 4. COS concentrations decreased with soil depth, with the opposite
228 trend for CO₂, consistent with the results reported above of soil surface COS uptake
229 and CO₂ emission at our orchard site. COS concentrations at depth of 2.5 cm was on
230 average 314 ppt, and about one-third lower than the mean surface, ambient, value of
231 460 ppt. The lowest COS concentration at depth of 20 cm (166 ppt) was almost one-
232 third of that at the soil surface. An exponential and a linear equations provided
233 reasonable fit to the changes in soil COS and CO₂ concentrations, respectively, as a
234 function of depth (z_{soil}):

$$235 \quad \begin{aligned} [COS] &= 283.5 \exp(-0.2z_{soil}) + 169.9, \quad R^2 = 0.99 \\ [CO_2] &= 122.2z_{soil} + 558.5, \quad R^2 = 0.99 \end{aligned} \quad (7)$$

236 In terms of individual site and campaign, all profiles except for BR in summer
237 (June) showed the general trend of decreasing [COS] and increasing [CO₂] with depth,
238 with the steepest gradient at the top 5 cm (Fig. 5). In the BR microsite in summer, CO₂

239 profiles were shallow, consistent with the low respiration (see July BR in Table 1). But
240 a decrease in COS concentration toward the surface, with surface value lower than the
241 next two soil depth points (Fig. 5J), was consistent with COS emission at that time (July
242 BR in Table 1).

243 As noted above, the profile data generally exhibited the steepest gradient at the top
244 few cm of the soil, indicating that the dominating COS sink (and likely also the CO₂
245 source) was located at shallow depth. We therefore used the gas concentration
246 difference at two shallowest depths ($z_{soil1} = 0$ and $z_{soil2} = 2.5$ cm) to provide an
247 approximation of the fluxes to and from the soil, to constrain the more extensive
248 chamber measurements. The COS diffusion coefficient, D_s , was estimated for each
249 campaigns (see Methods), indicating low D_s value in the UT site in June and July ($D_s =$
250 $2.55 \text{ mm}^2 \text{ s}^{-1}$), associated with the drip irrigation and the high soil water content, and
251 high values in the dryer soils ($D_s = 5.57 \text{ mm}^2 \text{ s}^{-1}$), with an average COS diffusion
252 coefficient of $4.40 \pm 0.29 \text{ mm}^2 \text{ s}^{-1}$. The soil COS flux estimates using the gradient
253 method is reported in Table 2. COS flux varied between -2.10 to +1.55 $\text{pmol m}^{-2} \text{ s}^{-1}$
254 with a mean value of $-1.02 \pm 0.26 \text{ pmol m}^{-2} \text{ s}^{-1}$ during the measurement periods,
255 consistent with the mean value of $-1.10 \pm 0.10 \text{ pmol m}^{-2} \text{ s}^{-1}$ reported above for the
256 chamber measurements. Also in agreement with the chamber measurements, fluxes at
257 UT and BT always showed COS uptake, with generally higher values in spring (March)
258 than in summer (May-June), while the BR data indicated change from uptake in spring
259 (March-April, -1.3 to -1.6 $\text{pmol m}^{-2} \text{ s}^{-1}$) to emission in June (+1.6 $\text{pmol m}^{-2} \text{ s}^{-1}$).

260

261 **3.4 Soil relative uptake**

262 Soil was always a source of CO₂ due respiration (combined autotrophic and
263 heterotrophic respiration). Soil CO₂ flux rates varied both spatially and temporally in
264 similar patterns to those of COS, and with overall range of +0.3 to +14.6 $\mu\text{mol m}^{-2} \text{ s}^{-1}$
265 (Table 1). The highest soil respiration values were observed in the UT sites in summer
266 (July, August; Table 1), with intermediate (+1 to about +3 $\mu\text{mol m}^{-2} \text{ s}^{-1}$) and low values
267 ($< +1 \mu\text{mol m}^{-2} \text{ s}^{-1}$) in the BT and BR sites, respectively. Generally, soil COS exchange

268 varied from release to increasing uptake with increasing CO₂ production in a non-linear
269 way (Fig. 6a). The normalized ratio of COS to CO₂ fluxes (SRU; Eq. 2) varied from -
270 1.92 to +1.85 with an average value of -0.37 ± 0.31 , with negative values indicating
271 COS uptake linked to CO₂ emission. SRU values showed response to both soil
272 temperature (Fig. 6b) and soil moisture (Fig. 6c), although with relatively low R² values.
273 Respiration increased with temperature while COS uptake declined and at temperature
274 above about 25 °C SRU turned positive when both COS and CO₂ are emitted from the
275 soil. SRU exhibited inverse relationships with soil moisture, with positive values in dry
276 soil and increasingly negative values with increasing soil moisture (Fig. 6c). Based on
277 its combined temperature (T_s) and moisture (θ) response, SRU could be forecasted by
278 the following algorithm, which explained 67% of the observed variations (Eq. 8):

$$279 \quad SRU = 0.01\exp(0.17T_s) - 0.02\theta - 1.00, R^2 = 0.67 \quad (8)$$

280 ANOVA analysis results indicated that SRU was not significantly different among
281 the three observation microsites (BR, BT, and UT; $P > 0.05$). Between the seasonal
282 campaigns, however, SRU values peaked in summer ($+0.53 \pm 0.66$) with highest
283 averaged soil temperature (29 °C) and was significantly higher than winter SRU (-1.44
284 ± 0.59) when soil temperature was lowest (11 °C; $P < 0.05$), and with no significant
285 difference in SRU among the other campaigns ($P > 0.05$).

286

287 **4. Discussions**

288 **4.1 Heterogeneity in soil COS exchange**

289 The observed soil-atmosphere COS exchange rates observed in this study (both
290 mean and range; Fig. 1, Table 1) are consistent with values reported in a range of other
291 ecosystems (-1.4 to -4.9 pmol m⁻² s⁻¹; Steinbacher et al., 2004; Kitz et al., 2017; White
292 et al., 2010; Berkelhammer et al., 2014), but lower than -11.0 to -11.8 pmol m⁻² s⁻¹ in a
293 riparian and subtropical forests (Berkelhammer et al., 2014; Yi et al., 2007). Soil COS
294 emissions were also observed in summer and spring campaigns, with maximal COS
295 emission consistent with the values of $+1.8$ to $+2.6$ pmol m⁻² s⁻¹ observed in a riparian
296 and alpine forests (Berkelhammer et al., 2014), but significantly lower than reported in

297 the senescing agricultural ecosystem ($\sim+30 \text{ pmol m}^{-2}\text{s}^{-1}$; Maseyk et al., 2014).

298 The observed range in the soil-atmosphere exchange fluxes reflected significant
299 heterogeneity on both the spatial and the temporal scales. The spatial scale
300 heterogeneity clearly reflected the contrasting microsite conditions with lower
301 temperatures and higher moisture under the trees (UT sites), compared with the higher
302 temperatures and lower moisture in exposed soil between rows (BR sites), with
303 intermediate, partially shaded, conditions between trees (BT sites). Indeed, a large
304 fraction of the variations in the COS flux ($\sim 75\%$) could be explained by a simple
305 algorithm as a function of these two variables, temperature and moisture. Note that
306 while temperature and θ co-varied in general, with high temperatures associated with
307 drier soil, under the wet UT conditions, sensitivity to temperature was significantly
308 reduced. In the dry soil conditions, emission was associated with high temperature, and
309 in the BR sites also with high solar radiation. However, all measurements were made
310 in dark chambers and could not involve photochemical production, which was also
311 demonstrated in agricultural soil by Kitz et al. (2017). Apparently even under dark
312 conditions, high temperature can induce high emission rates, as also noted when the
313 thermal insulation on the soil chamber in the BR site was incidentally removed and a
314 large spike in temperature ($52 \text{ }^\circ\text{C}$) and emission of $11.4 \text{ pmol m}^{-2} \text{ s}^{-1}$ was observed. Note
315 also that the soil profile results indicated that the emission source was below surface,
316 and maybe non-photochemical irrespective of the chamber opaques.

317 Temporal variations were observed both on the daily and seasonal time scales.
318 Diurnal changes were, however, minor compared to the changes from winter to summer
319 in all microsites. Shifts from uptake to emission were observed essentially only on the
320 seasonal time scale (Fig. 1). This likely reflected the dominance of soil moisture on the
321 COS flux rates. This is because θ did not change noticeably on the daily scale, while it
322 did change considerably across seasons (between 10.0 and 35.5% overall). Soil
323 temperatures did change over the daily cycle (e.g. 26.0 to $42.4 \text{ }^\circ\text{C}$ in the BR site during
324 summer), although such changes are still smaller than the seasonal changes in soil
325 temperature (e.g. 10.5 to $31.8 \text{ }^\circ\text{C}$ in the BR site). A dominant role of soil moisture in
326 explaining the variations in COS uptake is consistent with the results of Van Diest and

327 Kesselmeier (2008), but less so with the negligible θ effects in grassland under
328 simulated drought (Kitz et al., 2017).

329 COS uptake is thought to be related to carbonic anhydrase activity in soil
330 (Kesselmeier et al., 1999), which could be via microorganisms (Piazzetta et al., 2015),
331 such as Bacteria (Kamezaki et al., 2016; Kato et al., 2008), or fungi (Bunk et al., 2017;
332 Li et al., 2010; Masaki et al., 2016). CA activity is also influenced by soil moisture
333 (Davidson and Janssens, 2006; Seibt et al., 2006), although soil moisture can also
334 directly influence soil gas diffusion rates (Ogée et al., 2016; Sun et al., 2015). The effect
335 of CA on COS exchange can also be related to root distribution and the effects of CA
336 activity within plant roots (Seibt et al., 2006; Viktor and Cramer, 2005; Whelan and
337 Rhew, 2015). This could influence the spatial variations and soil moisture effects on
338 COS exchange in this study as most of the roots were distributed around the restricted
339 trees' drip irrigation zone at UT sites, and was sparse in the dryer areas, such as the BR
340 and BT sites (un-quantified observations).

341 At least part of the variations in soil COS fluxes could also reflect the differential
342 effects of environmental conditions on COS uptake and production process (Ogée et al.,
343 2016). Solubility in soil water (with COS solubility of 0.8 ml ml^{-1} ; Svoronos and Bruno,
344 2002) could also be significant, especially in the UT microsites, influenced by the drip
345 irrigation from May to September that could involve water percolation to deeper soil
346 layers. The drivers of soil COS production are still unclear. COS could be produced by
347 chemical processes in the lab (Ferm, 1957), but can also be produced by biotic process
348 in soils such as by hydrolysis of metallic thiocyanates (Katayama et al., 1992) with
349 thiocyanate hydrolase (Conrad, 1996; Svoronos and Bruno, 2002) and hydrolysis of
350 CS_2 (Cox et al., 2013; Smith and Kelly, 1988). Fungi are also reported to be the source
351 of COS (Masaki et al., 2016). Additionally, abiotic thermal degradation of organic
352 matter leading to COS production may be consistent with the temperature sensitivity of
353 COS emission in the BR microsite where biotic processes can be expected to be
354 minimized. Similar high temperature-dependent soil COS emissions were reported in
355 midlatitude forest (Commane et al., 2015) and agricultural field (Maseyk et al., 2014).
356 Lab incubation results also indicated thermal production of COS in soil with increasing

357 temperature (Liu et al., 2010; Whelan et al., 2016; Whelan and Rhew, 2015).
358 Photochemical production of soil COS was also proposed (Sun et al., 2015; Whelan
359 and Rhew, 2015), and assumed to be driven by ultraviolet fraction of incoming solar
360 radiation (Kitz et al., 2017). Note, however, that all measurements in the present study
361 were made in the dark. In addition, the chemical reaction of CO and MgSO₄ under
362 heating could also produce COS (Ferm, 1957). Note that MgSO₄ has been reported in
363 our study soil (Singer, 2007), and we observed relatively high CO concentration in our
364 field site (not shown due to insufficient calibration). Finally, the balance between the
365 uptake (likely biotic dominated) and emission (likely abiotically dominated) can also
366 be influenced by soil nitrogen (Kaisermann et al., 2018).

367

368 **4.2 Soil relative uptake**

369 We use SRU values to assess the relative importance of the soil COS flux
370 compared with the canopy, and indicate shifts from conservative links between
371 processes influencing COS and CO₂ (see Introduction). On average, the value of SRU
372 at our site was smaller than reported for riparian or pine forests (-0.37 vs -0.76 and -
373 1.08; Berkelhammer et al., 2014; Sun et al., 2018). This may reflect the contribution of
374 COS emissions at BR and BT in summer, that were not observed in the forest study.
375 Overall, the mean SRU values observed here indicated that the soil COS uptake flux
376 was proportionally less than 40% of the soil respiration flux. In contrast with the canopy
377 fluxes where the COS uptake flux is, proportionally, nearly twice as large as the CO₂
378 assimilation flux (LRU~1.6 at our site; Yang et al., 2018; 1.7 across vegetation types,
379 Whelan et al., 2018). In contrast to leaves with robust LRU value that tend toward a
380 constant, SRU at our site varied between -1.92 and +1.85. However, this range was
381 observed only in the dryer and exposed BR sites, while in the shaded and moist UT
382 sites, it was much narrower, -0.13 to -0.79. Furthermore, it seems that the high SRU
383 values (both positive and negative) represented conditions where the actual fluxes were
384 small (COS uptake was on average -3.0 in the UT but only 0.1 pmol m⁻² s⁻¹ in the BR
385 sites. It seems that the large SRU values in the BR microsites, were also associated with

386 low soil respiration, $0.5 \mu\text{mol m}^{-2} \text{s}^{-1}$ in BR sites, compared to $10 \mu\text{mol m}^{-2} \text{s}^{-1}$ in the
387 UT sites. It is therefore possible that the low SRU values are the more significant for
388 ecosystem scale studies and indicate a much smaller contribution to overall ecosystem
389 fluxes than that of the canopy (i.e., $\text{SRU} \sim -0.4$ vs $\text{LRU} \sim +1.7$).

390 Differential effects of changing environmental conditions on production and
391 uptake processes were reflected in relatively large spatial and temporal heterogeneity
392 observed in the soil COS exchange at our site. However, the contrasting effects of
393 production and emission may explain both the sharp increase in SRU values at high
394 temperatures as the effects of production counteract uptake (Fig. 6b), and the much
395 lower sensitivity to temperature of COS flux compared to that of CO_2 (Fig. 6a). Such
396 contrasting consumption/production effects may, in fact, reduce the magnitude of the
397 net flux of soil COS, and may explain the relatively narrow range of SRU values.

398 Application of COS as a tracer for canopy CO_2 exchange requires the accounting
399 for the soil effects and while knowledge of SRU can help predicting it, ultimately we
400 need to quantify the fluxes. Note in that respect, that in our recent canopy scale study
401 at the same site (Yang et al., 2018) indicated that in spite of the considerable variations
402 in soil COS fluxes, the soil COS uptake fluxes were equivalent to $\sim 1\%$ of the daytime
403 foliage flux across seasons, and reached $\sim 3\%$ in the spring peak season (but larger
404 proportions were observed during more stressful periods when fluxes were overall
405 small).

406

407 **4.3 Soil COS profiles**

408 Complementing our chamber measurements with soil profile measurements of
409 COS and CO_2 concentrations provided constrain on the relatively new surface soil COS
410 measurements and provided additional information on the possible location of the
411 source/sink in the soil. Using the near surface gradient yielded flux estimates
412 comparable to chamber measurements, providing a useful and rare quantitative
413 validation. For example, in May, the chamber and profile measurements were made at
414 about the same time (5th~9th May for chamber and 10th May for profile) and the

415 differences between chamber (all microsities) and gradient flux estimates, was
416 negligible ($\sim 0.2\text{-}0.6 \text{ pmol m}^{-2} \text{ s}^{-1}$). However, the profile results indicated in addition that
417 the sink/source activities concentrated at top soil layers, probably at around 5-10 cm
418 depth, as reflected in the minimum or maximum in gas concentrations (emphasizing
419 the need for high vertical resolution in employing the profile approach). The variable
420 profiles observed below these points must reflect temporal dynamics in the sink/source
421 activities across the profile. The near surface peak activity makes it particularly
422 sensitive to variations in temperature and moisture, as indeed observed (Figs. 2, 3). Low
423 COS concentration in the lower parts of the profile may result from continuous removal
424 of soil COS and may indicate distribution of CA activity beyond the litter layer and the
425 soil surface (Seibt et al., 2006). COS production, however, seems to occur only near the
426 soil surface with no indication for production in deeper layer, consistent with its high
427 temperature sensitivity, and not necessarily dependent on radiation (e.g. Kitz et al.,
428 2017).

429 Note that the gradient method based on the Fick's diffusion law have its own
430 limitations (Kowalski and Sánchezcañete, 2010; Sánchez-Cañete et al., 2017; Bekele et
431 al., 2007). However, it is simple low-cost approach and can help diagnose the
432 magnitude of soil fluxes, which can also help in identifying below ground processes
433 and their locations.

434

435 **5. Conclusions**

436 Our detailed analysis of the spatial and temporal variations in soil-atmosphere
437 exchange of COS provided new information on a key uncertainty in the application of
438 ecosystem COS flux to assess productivity. Furthermore, we provide validation of the
439 surface chamber measurements that are generally in use, by the additional gradient
440 approach. Our results show that both microsities and seasonal variations in COS fluxes
441 were related to soil moisture, temperature, and the distance from the tree (likely
442 reflecting root distribution), but we suggest that soil moisture is the predominant
443 environmental control over soil COS exchanges at our site. A simple algorithm was
444 sufficient to forecast most of the variations in soil COS flux supporting its incorporated

445 into ecosystem scale applications, as we recently demonstrated in a parallel study at the
446 same site (Yang et al., 2018).

447 Clearly, uncertainties are still associated with soil processes involving COS, the
448 differential effects of soil moisture, temperature, and communities of microorganisms
449 and are likely to contribute to both the spatial and temporal variations in soil net COS
450 exchange and require further research.

451

452 **Author contributions:**

453 DY designed the study; FY, RQ, FT, RS and DY performed the experiments. FY
454 and FT analyzed the data. DY and FY wrote the paper with discussions and
455 contributions to interpretations of the results from all co-authors.

456

457 **Acknowledgements**

458 We are grateful to Omri Garini, Madi Amer, and Boaz Ninyo-Setter for their help. This work
459 was supported by the Minerva foundation, a joint NSFC-ISF grant 2579/16; Israel Science
460 Foundation (ISF 1976/17), the German Research Foundation (DFG) as part of the CliFF
461 Project, and the JNF-KKL. FY is supported by the National Natural Science Foundation of
462 China (41775105), and the Natural Science Foundation of Gansu Province (17JR5RA341).

463 **References**

- 464 Asaf, D., Rotenberg, E., Tatarinov, F., Dicken, U., Montzka, S. A., and Yakir, D.:
465 Ecosystem photosynthesis inferred from measurements of carbonyl sulphide flux,
466 Nat. Geosci., 6, 186-190, 2013.
- 467 Bekele, A., Kellman, L., and Beltrami, H.: Soil Profile CO₂ concentrations in forested
468 and clear cut sites in Nova Scotia, Canada, Forest. Ecol. Manag., 242, 587-597,
469 2007.
- 470 Berkelhammer, M., Asaf, D., Still, C., Montzka, S., Noone, D., Gupta, M., Provencal,
471 R., Chen, H., and Yakir, D.: Constraining surface carbon fluxes using in situ
472 measurements of carbonyl sulfide and carbon dioxide, Global Biogeochem. Cy.,
473 28, 161-179, 2014.
- 474 Berry, J., Wolf, A., Campbell, J. E., Baker, I., Blake, N., Blake, D., Denning, A. S.,
475 Kawa, S. R., Montzka, S. A., and Seibt, U.: A coupled model of the global cycles
476 of carbonyl sulfide and CO₂: A possible new window on the carbon cycle, J.
477 Geophys. Res.:Biogeo., 118, 842-852, 2013.
- 478 Bunk, R., Behrendt, T., Yi, Z., Andreae, M. O., and Kesselmeier, J.: Exchange of
479 carbonyl sulfide (OCS) between soils and atmosphere under various CO₂
480 concentrations, J. Geophys. Res.:Biogeo., 122, 1343-1358, 2017.
- 481 Commane, R., Meredith, L. K., Baker, I. T., Berry, J. A., Munger, J. W., Montzka, S. A.,
482 Templer, P. H., Juice, S. M., Zahniser, M. S., and Wofsy, S. C.: Seasonal fluxes of
483 carbonyl sulfide in a midlatitude forest, P. Natl. Acad. Sci. U.S.A., 112, 14162-
484 14167, 2015.
- 485 Conrad, R.: Soil microorganisms as controllers of atmospheric trace gases (H₂, CO,
486 CH₄, OCS, N₂O, and NO), Microbiol. Rev., 60, 609-640, 1996.
- 487 Cox, S. F., McKinley, J. D., Ferguson, A. S., O'Sullivan, G., and Kalin, R. M.:
488 Degradation of carbon disulphide (CS₂) in soils and groundwater from a CS₂-
489 contaminated site, Environ. Earth Sci., 68, 1935-1944, 2013.
- 490 Davidson, E. A., and Janssens, I. A.: Temperature sensitivity of soil carbon
491 decomposition and feedbacks to climate change, Nature, 440, 165-173, 2006.
- 492 Ferm, R. J.: The chemistry of carbonyl sulfide, Chemical Reviews, 57, 621-640, 1957.

493 Jones H G . Plants and Microclimate: A Quantitative Approach to Environmental Plant
494 Physiology, Cambridge University Press, 1983.

495 Kaisermann, A., Ogée, J., Sauze, J., Wohl, S., Jones, S. P., Gutierrez, A., and Wingate,
496 L.: Disentangling the rates of carbonyl sulfide (COS) production and consumption
497 and their dependency on soil properties across biomes and land use types, *Atmos.*
498 *Chem. Phys.*, 18, 9425-9440, 2018.

499 Kamezaki, K., Hattori, S., Ogawa, T., Toyoda, S., Kato, H., Katayama, Y., and Yoshida,
500 N.: Sulfur Isotopic Fractionation of Carbonyl Sulfide during Degradation by Soil
501 Bacteria, *Environ. Sci. Technol.*, 50, 3537-3544, 2016.

502 Kapiluto, Y., Dan, Y., Tans, P., and Berkowitz, B.: Experimental and numerical studies
503 of the ¹⁸O exchange between CO₂ and water in the atmosphere–soil invasion flux,
504 *Geochim. Cosmochim. Ac.*, 71, 2657-2671, 2007.

505 Katayama, Y., Narahara, Y., Inoue, Y., Amano, F., Kanagawa, T., and Kuraishi, H.: A
506 thiocyanate hydrolase of *Thiobacillus thioparus*. A novel enzyme catalyzing the
507 formation of carbonyl sulfide from thiocyanate, *J. Biol. Chem.*, 267, 9170-9175,
508 1992.

509 Kato, H., Saito, M., Nagahata, Y., and Katayama, Y.: Degradation of ambient carbonyl
510 sulfide by *Mycobacterium* spp. in soil, *Microbiology+*. 154, 249-255, 2008.

511 Kesselmeier, J., Teusch, N., and Kuhn, U.: Controlling variables for the uptake of
512 atmospheric carbonyl sulfide by soil, *J. Geophys. Res.: Atmos.*, 104, 11577-11584,
513 1999.

514 Kitz, F., Gerdel, K., Hammerle, A., Laterza, T., Spielmann, F. M., and Wohlfahrt, G.: In
515 situ soil COS exchange of a temperate mountain grassland under simulated
516 drought, *Oecologia*, 183, 851-860, 2017.

517 Kooijmans L.M.J., Uitslag N.A.M., Zahnister M.S., Nelson D.D., Motzka S.A. and
518 Chen H.: Continuous and high precision atmospheric concentration measurements
519 of COS, CO₂, CO and H₂O using a quantum cascade laser spectrometer (QCLS).
520 *Atmos. Meas. Tech.*, 9, 5293-5314, 2016

521 Kowalski, A. S., and Sánchezcañete, E. P.: A New Definition of the Virtual Temperature,
522 Valid for the Atmosphere and the CO₂-Rich Air of the Vadose Zone, *J. Appl.*

523 Meteorol. Clim., 49, 1238-1242, 2010.

524 Kuhn, U., Ammann, C., Wolf, A., Meixner, F., Andreae, M., and Kesselmeier, J.:
525 Carbonyl sulfide exchange on an ecosystem scale: Soil represents a dominant sink
526 for atmospheric COS, Atmos. Environ., 33, 995-1008, 1999.

527 Li, X., Liu, J., and Yang, J.: Variation of H₂S and COS emission fluxes from
528 Calamagrostis angustifolia Wetlands in Sanjiang Plain, Northeast China, Atmos.
529 Environ., 40, 6303-6312, 2006.

530 Li, X. S., Sato, T., Ooiwa, Y., Kusumi, A., Gu, J. D., and Katayama, Y.: Oxidation of
531 elemental sulfur by Fusarium solani strain THIF01 harboring endobacterium
532 Bradyrhizobium sp, Microb. Ecol., 60, 96-104, 2010.

533 Liu, J., Geng, C., Mu, Y., Zhang, Y., Xu, Z., and Wu, H.: Exchange of carbonyl sulfide
534 (COS) between the atmosphere and various soils in China, Biogeosciences, 7, 753-
535 762, 2010.

536 Masaki, Y., Ozawa, R., Kageyama, K., and Katayama, Y.: Degradation and emission of
537 carbonyl sulfide, an atmospheric trace gas, by fungi isolated from forest soil,
538 FEMS Microbiol. Lett., 363, fnw197, 2016.

539 Maseyk, K., Berry, J. A., Billesbach, D., Campbell, J. E., Torn, M. S., Zahniser, M., and
540 Seibt, U.: Sources and sinks of carbonyl sulfide in an agricultural field in the
541 Southern Great Plains, P. Natl. Acad. Sci. U.S.A., 111, 9064-9069, 2014.

542 Ogée, J., Sauze, J., Kesselmeier, J., Genty, B., Van Diest, H., Launois, T., and Wingate,
543 L.: A new mechanistic framework to predict OCS fluxes from soils,
544 Biogeosciences, 13, 2221-2240, 2016.

545 Penman, H. L.: Gas and Vapor Movements in the Soli: I. The diffusion of vapors
546 through porous solids, J. Agric. Sci., 30, 437-462, 1940.

547 Piazzetta, P., Marino, T., and Russo, N.: The working mechanism of the beta-carbonic
548 anhydrase degrading carbonyl sulphide (COSase): a theoretical study, Phys. Chem.
549 Chem. Phys., 17, 14843-14848, 2015.

550 Sánchez-Cañete, E. P., Scott, R. L., Van Haren, J., and Barron-Gafford, G. A.:
551 Improving the accuracy of the gradient method for determining soil carbon dioxide
552 efflux, J. Geophys. Res.:Biogeo., 122, 2017.

553 Seibt, U., Kesselmeier, J., Sandoval-Soto, L., Kuhn, U., and Berry, J.: A kinetic analysis
554 of leaf uptake of COS and its relation to transpiration, photosynthesis and carbon
555 isotope fractionation, *Biogeosciences*, 7, 333-341, 2010.

556 Seibt, U., Wingate, L., Lloyd, J., and Berry, J. A.: Diurnally variable $\delta^{18}\text{O}$ signatures of
557 soil CO_2 fluxes indicate carbonic anhydrase activity in a forest soil, *J. Geophys.*
558 *Res.: Atmos.*, 111, G04005, 2006.

559 Singer, A.: *The soils of Israel*, Springer Science & Business Media, 2007.

560 Smith, N. A., and Kelly, D. P.: Oxidation of carbon disulphide as the sole source of
561 energy for the autotrophic growth of *Thiobacillus thioparus* strain TK-m,
562 *Microbiology+*. 134, 3041-3048, 1988.

563 Steinbacher, M., Bingemer, H. G., and Schmidt, U.: Measurements of the exchange of
564 carbonyl sulfide (OCS) and carbon disulfide (CS_2) between soil and atmosphere
565 in a spruce forest in central Germany, *Atmos. Environ.*, 38, 6043-6052, 2004.

566 Sun, W., Maseyk, K., Lett, C., and Seibt, U.: A soil diffusion–reaction model for surface
567 COS flux: COSSM v1, *Geosci. Model. Dev.*, 8, 3055-3070, 2015.

568 Sun, W., Kooijmans, L. M. J., Maseyk, K., Chen, H., Mammarella, I., Vesala, T., Levula,
569 J., Keskinen, H., and Seibt, U.: Soil fluxes of carbonyl sulfide (COS), carbon
570 monoxide, and carbon dioxide in a boreal forest in southern Finland, *Atmos. Chem.*
571 *Phys.*, 18, 1363-1378, 2018.

572 Svoronos, P. D., and Bruno, T. J.: Carbonyl sulfide: a review of its chemistry and
573 properties, *Ind. Eng. Chem. Res.*, 41, 5321-5336, 2002.

574 Van Diest, H., and Kesselmeier, J.: Soil atmosphere exchange of carbonyl sulfide (COS)
575 regulated by diffusivity depending on water-filled pore space, *Biogeosciences*, 5,
576 475-483, 2008.

577 Viktor, A., and Cramer, M. D.: The influence of root assimilated inorganic carbon on
578 nitrogen acquisition/assimilation and carbon partitioning, *New Phytol.*, 165, 157-
579 169, 2005.

580 Wehr, R., Commane, R., Munger, J. W., McManus, J. B., Nelson, D. D., Zahniser, M.
581 S., Saleska, S. R., and Wofsy, S. C.: Dynamics of canopy stomatal conductance,
582 transpiration, and evaporation in a temperate deciduous forest, validated by

583 carbonyl sulfide uptake, *Biogeosciences*, 14, 389, 2017.

584 Whelan, M. E., Min, D.-H., and Rhew, R. C.: Salt marsh vegetation as a carbonyl sulfide
585 (COS) source to the atmosphere, *Atmos. Environ.*, 73, 131-137, 2013.

586 Whelan, M. E., and Rhew, R. C.: Carbonyl sulfide produced by abiotic thermal and
587 photodegradation of soil organic matter from wheat field substrate, *J. Geophys.*
588 *Res.:Biogeo.*, 120, 54-62, 2015.

589 Whelan, M. E., Hilton, T. W., Berry, J. A., Berkelhammer, M., Desai, A. R., and
590 Campbell, J. E.: Carbonyl sulfide exchange in soils for better estimates of
591 ecosystem carbon uptake, *Atmos. Chem. Phys.*, 16, 3711-3726, 2016.

592 Whelan, M. E., Lennartz, S. T., Gimeno, T. E., Wehr, R., Wohlfahrt, G., Wang, Y.,
593 Kooijmans, L. M. J., Hilton, T. W., Belviso, S., Peylin, P., Commane, R., Sun, W.,
594 Chen, H., Kuai, L., Mammarella, I., Maseyk, K., Berkelhammer, M., Li, K. F.,
595 Yakir, D., Zumkehr, A., Katayama, Y., Ogée, J., Spielmann, F. M., Kitz, F., Rastogi,
596 B., Kesselmeier, J., Marshall, J., Erkkilä, K. M., Wingate, L., Meredith, L. K., He,
597 W., Bunk, R., Launois, T., Vesala, T., Schmidt, J. A., Fichot, C. G., Seibt, U.,
598 Saleska, S., Saltzman, E. S., Montzka, S. A., Berry, J. A., and Campbell, J. E.:
599 Reviews and syntheses: Carbonyl sulfide as a multi-scale tracer for carbon and
600 water cycles, *Biogeosciences*, 15, 3625-3657, 2018.

601 White, M., Zhou, Y., Russo, R., Mao, H., Talbot, R., Varner, R., and Sive, B.: Carbonyl
602 sulfide exchange in a temperate loblolly pine forest grown under ambient and
603 elevated CO₂, *Atmos. Chem. Phys.*, 10, 547-561, 2010.

604 Yang, F., Qubaja, R., Tatarinov, F., Rotenberg, E., and Yakir, D.: Assessing canopy
605 performance using carbonyl sulfide measurements, *Glob. Change Biol.*, 24, 3486-
606 3498, 2018.

607 Yi, Z., Wang, X., Sheng, G., Zhang, D., Zhou, G., and Fu, J.: Soil uptake of carbonyl
608 sulfide in subtropical forests with different successional stages in south China, *J.*
609 *Geophys. Res.: Atmos.*, 112, D08302, 2007.

610 **Figure captions:**

611 **Figure 1.** Spatial variability of soil COS flux at three sites, between trees (a), between
612 rows (b), and under tree (c). Each figure shows the diurnal cycling of soil COS flux in
613 the four campaigns. Each data point was the hourly mean \pm 1 S.E. (N=3).

614 **Figure 2.** Relationship of soil COS flux and soil moisture. Each data point represents
615 the diurnal average (n=24) for each microsite and season (measurement campaign).
616 Error bars represent \pm 1 S.E. around the mean; errors for flux are about the size of the
617 symbols.

618 **Figure 3.** Soil COS flux as a function of temperature and its linear regression line.
619 Each data point represents the diurnal average (n=24) for each site and season
620 (campaign). Error bars represent \pm 1 S.E. around the mean. The data point marked in
621 black circle were collected during irrigation cycle (enhanced uptake) and were excluded
622 from the regression.

623 **Figure 4.** Mean COS and CO₂ concentrations at different soil depth. The COS
624 concentration decreases exponentially with soil depth. The data point is the mean of the
625 combined data at each of the four measurement campaigns (N=4; \pm 1 S.E.).

626 **Figure 5.** Soil COS and CO₂ concentration profiles at the three microsities in four
627 measurement campaigns. The data points are the mean of all measurements in a
628 campaign (N=4, \pm 1 S.E.)

629 **Figure 6.** The relationships between soil COS and CO₂ flux rates (chamber
630 measurements; a). The response of soil relative uptake (SRU; normalized ratio of COS
631 to CO₂ fluxes) to soil temperature (b) and to soil water content (c). The data points
632 represent the diurnal average (N=24) of each site and season (measurement campaign).
633 Error bars represent \pm 1 S.E. around the mean (often the size of the symbol).

634 **Table 1.** Mean values of soil COS and CO₂ flux rates across sites (BR, between rows;
635 BT, between trees; UT, under tree), and seasons, together with the normalized ratio of
636 COS/CO₂ fluxes (SRU), and the mean soil temperature at 5 cm depth (*T_s*) and soil water
637 content (% by wt; *θ*).

Campaigns	Sites	COS flux (pmol m ⁻² s ⁻¹)	CO ₂ flux (μmol m ⁻² s ⁻¹)	SRU	<i>T_s</i> (°C)	<i>θ</i> (%)
August, 2015	BR	1.83±0.08	0.77±0.04	1.85	31.66±1.01	9.98±0.28
	BT	0.06±0.05	3.33±0.05	0.01	29.09±0.20	19.77±0.02
	UT	-3.64±0.13	10.79±0.12	-0.26	28.80±0.26	24.03±0.40
December, 2015	BR	-0.74±0.07	0.30±0.02	-1.92	10.50±0.17	23.33±1.89
	BT	-2.52±0.10	1.21±0.03	-1.62	11.20±0.19	24.22±0.94
	UT	-3.87±0.08	3.81±0.07	-0.79	12.17±0.16	26.11±1.01
May, 2016	BR	-0.77±0.02	0.32±0.02	-1.88	21.67±0.32	15.56±0.38
	BT	-0.05±0.04	1.31±0.05	-0.03	22.20±0.34	15.70±1.03
	UT	-1.80±0.11	10.78±0.54	-0.13	20.35±0.38	22.11±1.44
July, 2016	BR	0.21±0.04	0.79±0.05	0.21	29.66±0.60	14.73±0.57
	BT	0.76±0.09	1.97±0.04	0.30	26.68±0.15	17.49±0.70
	UT	-2.67±0.09	14.58±0.40	-0.14	27.83±0.34	35.47±3.47

638

639 **Table 2.** Estimates of soil COS and CO₂ fluxes from soil concentration gradient measurements (*T_s*, soil temperature; *θ*, soil water content; BR,
640 between rows; BT, between trees; UT, under tree.)

Campaigns	Sites	COS flux (pmol m ⁻² s ⁻¹)	CO ₂ flux (μmol m ⁻² s ⁻¹)	CO ₂ diffusion coefficient (mm ² s ⁻¹)	COS diffusion coefficient (mm ² s ⁻¹)	<i>T_s</i> (°C)	<i>θ</i> (%)
March, 2016	BR	-1.31	2.34	5.21	4.40	17.9	19.4
	BT	-1.15	2.21	4.80	4.05	16.2	21.8
	UT	-2.10	5.89	4.76	4.02	17.3	22.4
April, 2016	BR	-1.55	1.07	6.66	5.62	23.0	11.0
	BT	-0.89	1.14	6.44	5.43	20.4	11.6
	UT	-1.74	4.73	6.01	5.07	22.4	15.2
May, 2016	BR	-0.98	2.21	5.68	4.79	21.9	17.4
	BT	-0.51	1.24	5.06	4.27	22.0	21.6
	UT	-1.20	11.36	3.11	2.63	20.1	34.5
June, 2016	BR	1.55	2.63	6.61	5.57	35.9	15.5
	BT	-1.17	2.60	5.20	4.39	26.3	21.7
	UT	-1.19	11.85	3.02	2.55	22.9	35.6

641

Figure 1

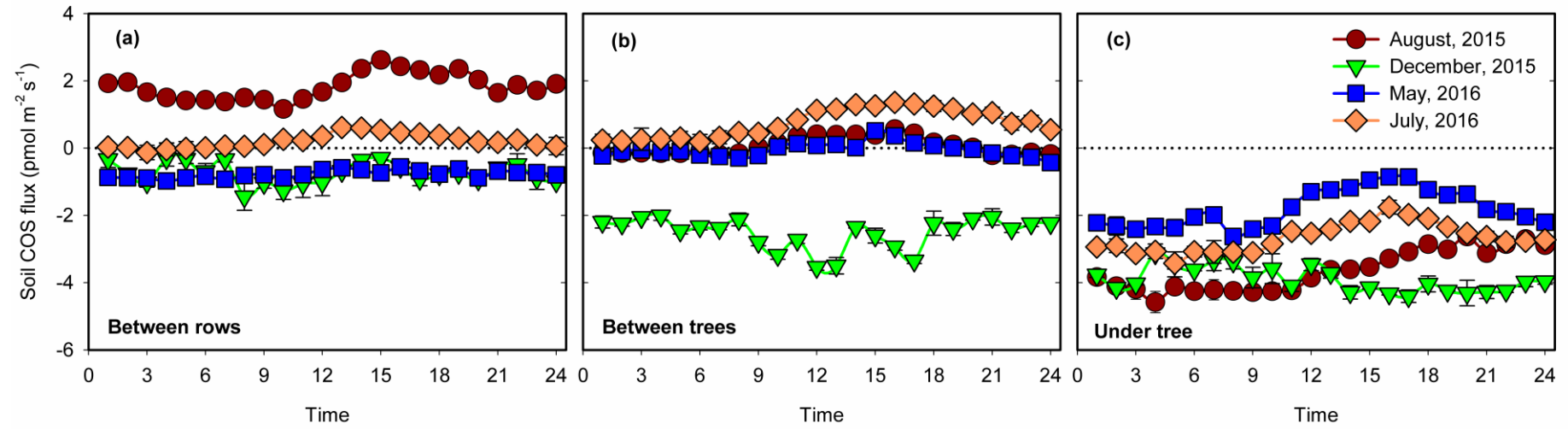


Figure 2

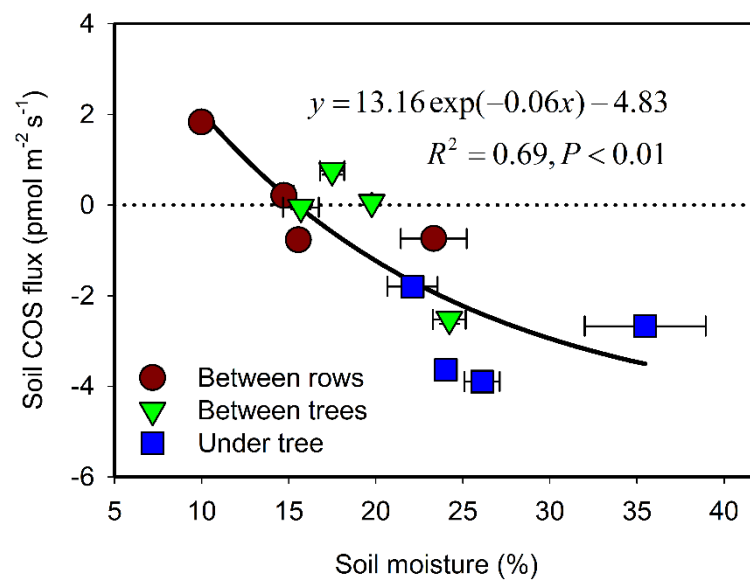


Figure 3

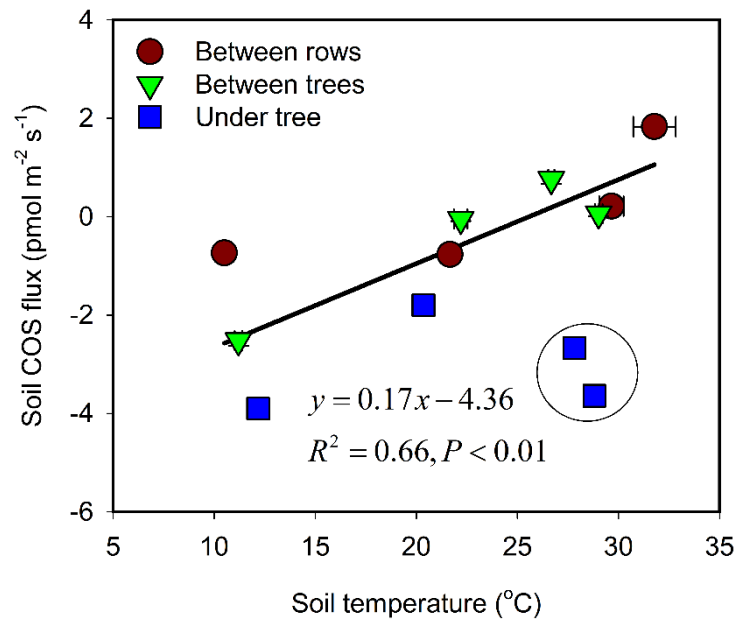


Figure 4

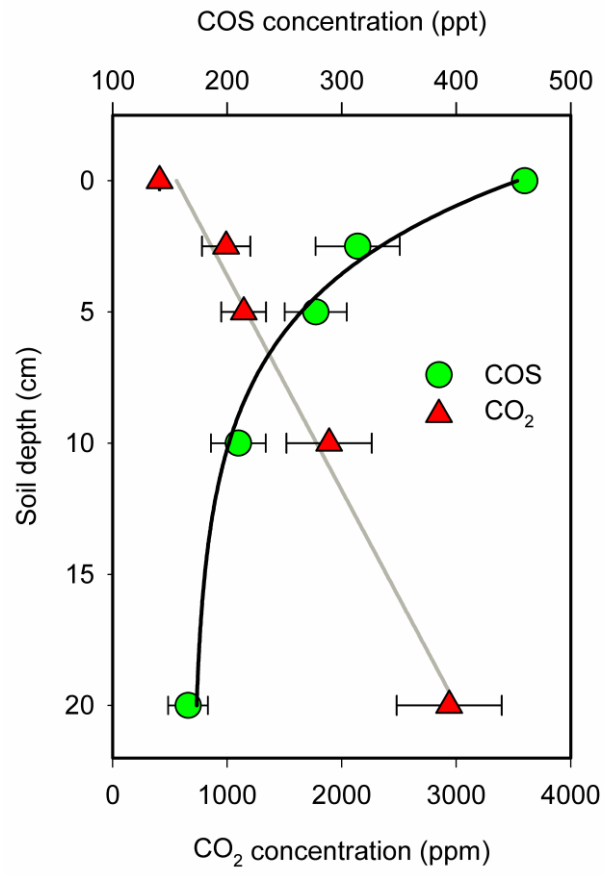


Figure 5

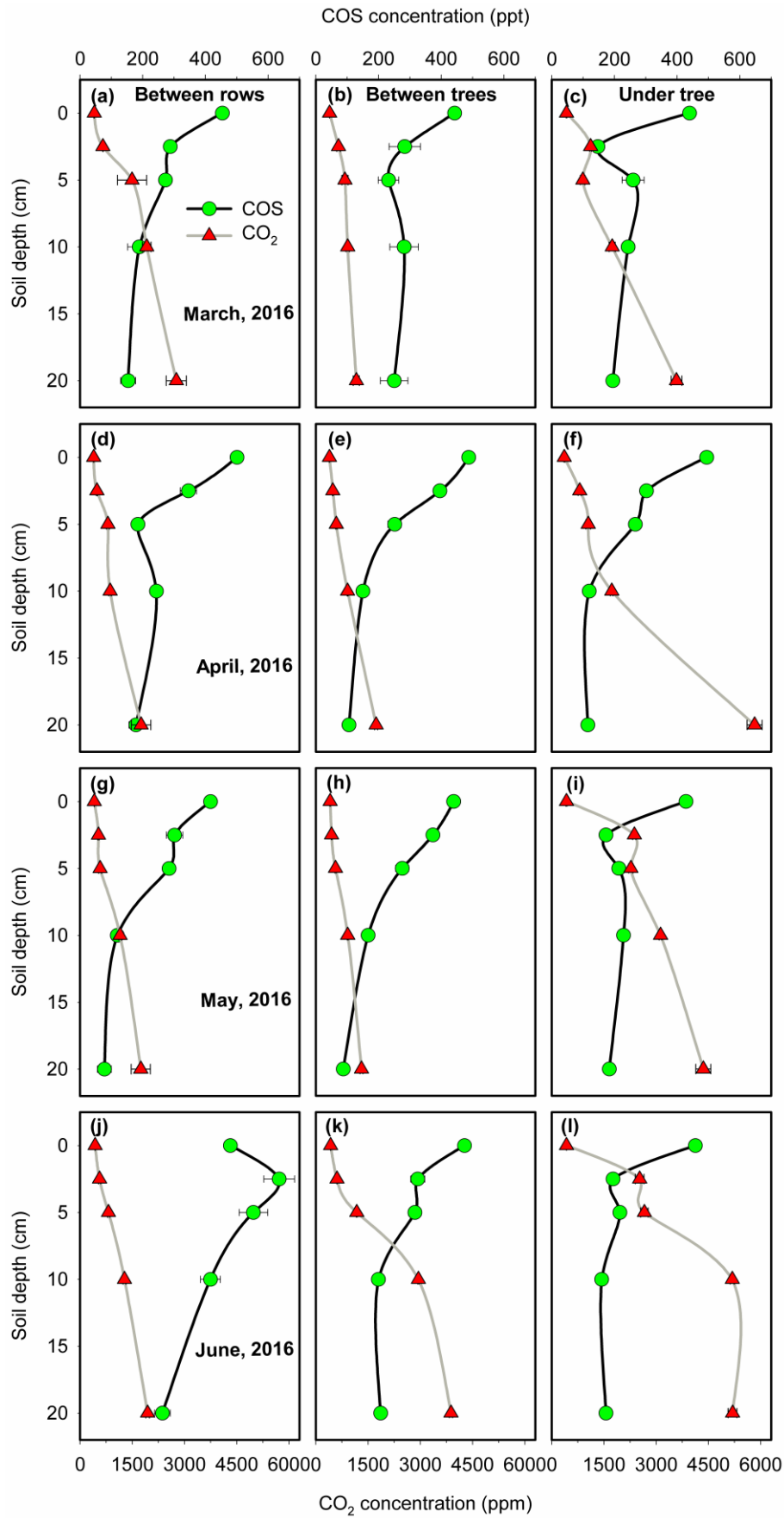


Figure 6

